Electrical conductivity of magnetically stabilized fluidized-bed electrodes – Chronoamperometric and impedance studies

André Tschöpe[a], Stefan Heikenwälder[a], Michael Schneider[b], Karl Mandel[b,c], Matthias Franzreb[a,*]

[a] Institute of Functional Interfaces, Karlsruhe Institute of Technology, Hermann-von-Helmholtz-Platz 1, 76344 Eggenstein-Leopoldshafen, Germany
[b] Fraunhofer Institute for Silicate Research ISC, Neunerplatz 2, 97082 Wuerzburg, Germany
[c] Department of Chemistry and Pharmacy, Inorganic Chemistry, Friedrich-Alexander University Erlangen-Nürnberg (FAU), Egerlandstrasse 1, 91058 Erlangen, Germany

HIGHLIGHTS

- Improved charge transport within a fluidized bed electrode by a superimposed magnetic field.
- Doubling of the specific conductivity in close proximity to the working electrode.
- Enhancement of the effective capacity and effective electrode surface by up to 400%.

ARTICLE INFO

Keywords:
Electrochemical reactor
Particle electrode
Magnetically stabilized fluidized bed
Electrochemical impedance spectroscopy
Magnetically stabilized electrode

ABSTRACT

Fluidized-bed electrodes could offer an interesting way to increase the electrode surface area applicable in electrochemical processes when the problem of poor electrical contact within the particle bed could be overcome. We recently demonstrated, that the contacting can be improved by the use of magnetizable electrode particles and the superposition of a magnetic field. However, details of the magnetic influence on the charge transport are still mostly unknown. In this work, we investigate the electrodynamics of a fluidized bed electrode with and without the superposition of a magnetic field by means of chronoamperometry and electrochemical impedance spectroscopy (EIS). In the chronoamperometric studies two types of charge transfer mechanism can be distinguished by the slope of the resistance increase with increasing distance between the electrodes. In close proximity to the electrodes direct conductive charge transfer along statistically formed particle chains dominates. Because the probability of uninterrupted particle chains quickly diminishes with increasing length, above a certain distance of approx. 6 mm a second, so-called convective, charge transfer mechanism dominates. This mechanism is based on the transfer of electrons between colliding fluidized particles and corresponds with a substantially higher specific resistance. The conductive charge transfer mechanism can be enhanced by up to a factor of four applying a superimposed magnetic field, while the second mechanism shows only a weak field dependence. The presented equivalent circuit model and the magnetic field dependency of its parameters contribute to a deeper understanding of the novel magnetically stabilized fluidized bed electrode and demonstrate the usefulness of EIS measurements for the prediction of the effectiveness of a particle based electrochemical reactor.

1. Introduction

Conversion rates in electrochemical processes can be increased by maximizing the ratio of electrode surface to solution volume. Here, the parameter of the effective electrode surface per electrode volume is an important influencing factor [1]. Fine particle based electrodes can maximize this ratio and increase the electrode surface area involved in the electrochemical conversion [1,2]. The so called “fluidized bed electrode” is based on fluidized fine particles and combines the advantages of large specific surfaces, tolerance to suspended solids and low pressure drops within an electrochemical process [3,4]. However, electrochemical processes, in which fluidized bed electrodes are used, pose difficulties in contacting the individual electrode particles with each other and with the current source [3,5 7]. Here the contacting of the electrode particles depends on the expansion state of the fluidized bed, so that with a stronger expansion, which follows with a higher flow rate, the particle contacting is reduced [3,5,8]. Consequently, with stronger expansion of the electrode bed, the resistance of the fluidized

* Corresponding author.
E-mail addresses: andre.tschoepe@kit.edu (A. Tschöpe), matthias.franzreb@kit.edu (M. Franzreb).

bed electrode also increases over the bed length, resulting in a stronger potential drop and only a part of the electrode bed can be used for the electrochemical reaction process [9,10].

A possibility to improve the contacting of the electrode particles within a fluidized bed electrode with each other as well as with the current source was investigated in a previous paper [11]. In this work, a magnetically stabilized fluidized bed [12 14] was combined with an electrochemical fluidized bed electrode for the first time. Here, an electric coil was placed around the electrochemical reaction system in order to influence the magnetic electrode particles in the system and to enhance the contacting. During the reaction process, a static axis symmetric magnetic field was generated by means of a DC voltage so that the fluidized magnetic electrode particles could be aligned along the magnetic field lines. This suppressed the uncontrolled movements of the electrode particles and simultaneously improved particle particle contact and particle electrode contact. With electrode particles consisting of a composite material of activated carbon, conductive carbon black and magnetite [15], it could be shown in an electrochemical model process that the electrochemical conversion could be improved by up to 100% by superposition of a magnetic field of 20 mT [11]. At the same time, the magnetic field increased the effective electrode surface participating in the electrochemical conversion by up to 400% [11]. In general, the mentioned paper showed that the superposition of the magnetic field on the fluidized bed electrode has improved the contacting of the electrode particles with each other as well as the electrochemical conversion in a redox reaction process, but more detailed investigations of the conductivity and charge transport within a magnetically influenced fluidized bed electrode have not yet been conducted.

In contrast, several studies investigating the potential distribution and conductivity of a conventional fluidized bed electrode, have already been carried out by different authors [3,5,6,9,10,16,17]. These investigations are mostly based on Newman and Tobias's [18] model of a porous electrode, which describes the fluidized bed electrode as a system of two pseudo continuous phases with different conductivities. Here a fluidized bed electrode consists of a phase of the electrode particles and the electrolyte solution in which the particles are fluidized [1,19]. All these investigations showed the important influence of the electrical conductivity of the dispersed phase of the fluidized bed electrode, which influences the potential distribution within the bed. Thereby the conduction mechanism depends on the fluidization and expansion of the fluidized bed. Fleischmann and Sabacky presented two conductivity mechanisms, the convective and the conductive mechanism, which are mainly responsible for the charge transport within a fluidized bed electrode [5,9]. According to Sabacky, the charge transport in the fluidized bed is mainly caused by the direct contact of the particles with the current source, as well as with particles that are in contact with the current source [5]. Here the charge transport depends on randomly formed particle chains within the electrode bed and represents the conductive mechanism. Fleischmann, on the other hand, suggests that the capacitive charge effect has the main influence on the charge transport within a fluidized bed electrode [9]. Here the electrical double layer of the particles can be charged by the random contact of the electrode particles with the current source [5,9]. Furthermore, the charged particles can move to another part in the electrode bed and share their charge in contact with other particles [5]. If the potential difference between the charged particle and the surrounding solution is high enough, the electrode particles can also be discharged by means of an electrochemical reaction.

Very few dynamic analyses of the charge transport within a fluidized bed electrode, have been reported so far. One reason is that on a microscopic level a fluidized bed electrode is not in a steady state condition and constantly changes during the application process due to the particle movements in the electrode bed [1,19,20]. Nevertheless, electrochemical impedance spectroscopy (EIS) is a powerful tool that is able to deliver valuable information about the electrochemical and electric properties of the electrode and the electrolyte [21]. The first resistance measurements, which were carried out with electrochemical impedance spectroscopy, have been performed by Huh and Evans [22,23]. However, these authors could not find any significant differences in the impedance in relation to the frequency and could only identify the influence of the bed expansion onto the resistance. Gabrielli et al. [1] investigated the dynamic behavior of the fluidized bed electrode at different expansion states in order to study the particle particle contact, the solution resistance and the electrical double layer. At the same time Gabrielli et al. [1] proposed a first model describing the behavior of the charge transport in a fluidized bed with non porous gold plated electrode particles [1,19].

In this work, we investigate the electrodynamics of a fluidized bed electrode with and without the superposition of a magnetic field by means of DC chronoamperometry and electrochemical impedance spectroscopy (EIS). The application of these complementary characterization techniques enables us to study different mechanism of charge transfer within the fluidized bed and to focus on different regions of the bed. On the basis of the data from the characterization techniques, this work discusses in detail the influence of the magnetic field on the conductivity and on the basics of charge transport within a fluidized bed electrode. By this, different phenomena of the magnetic influence on the electrochemical conversion within a fluidized bed electrochemical reactor can be explained. Therefore, while our previous paper [11] gave the proof of concept of an enhanced electrochemical productivity of a fluidized bed particle electrode when a magnetic field is superposed, the present work shows the reasons and limitations of this effect. At the end we demonstrate, that the findings which can be extracted from the fast and easy to conduct characterization techniques, give valuable information about the performance increase which can be expected when superposing a fluidized bed electrode within an electrochemical reactor by a magnetic field.

2. Material and methods

2.1. Chemicals and solutions

All chemicals were analytical grade and used without further purification. Water used for all experiments was produced using a Milli Q Ultrapure system from the company Merck Millipore (Billerica, USA). Sodium chloride was purchased from Merck (Darmstadt, Germany). The processed resin for the 3D printed components of the reactor device was VeroClear (mainly composed of polymethylmethacrylat (PMMA)) from the company Stratasys (Edina, USA).

2.2. Magnetic electrode particles

The magnetic electrode particles, that were used to expand the electrode surface, consisted of activated carbon, conductive carbon black and magnetite (Fig. 1A). The volumetric particle size distribution of these particles is plotted in Fig. 1B, showing a mean particle size of approximately 175 μm. The shape of the electrode particles was largely non spherical. A more detailed description of the particles and their synthesis can be found in [11,15]. For further characterization the specific resistance of a dry, gently compressed particle bed (Fig. 1C) as well as the magnetization curve (Fig. 1D) of the electrode particles were determined.

2.3. Magnetically stabilized fluidized bed reactor

2.3.1. Fluidized bed reactor

The housing of the developed magnetically stabilized fluidized bed reactor was designed using the CAD Software Inventor 2020 (Autodesk, San Rafael, USA) and manufactured using a 3D printer (Objet Eden260VS, Stratasys, MN, USA). The reactor consists of three main components, which can be assembled using tri clamps (Bio Clamp,

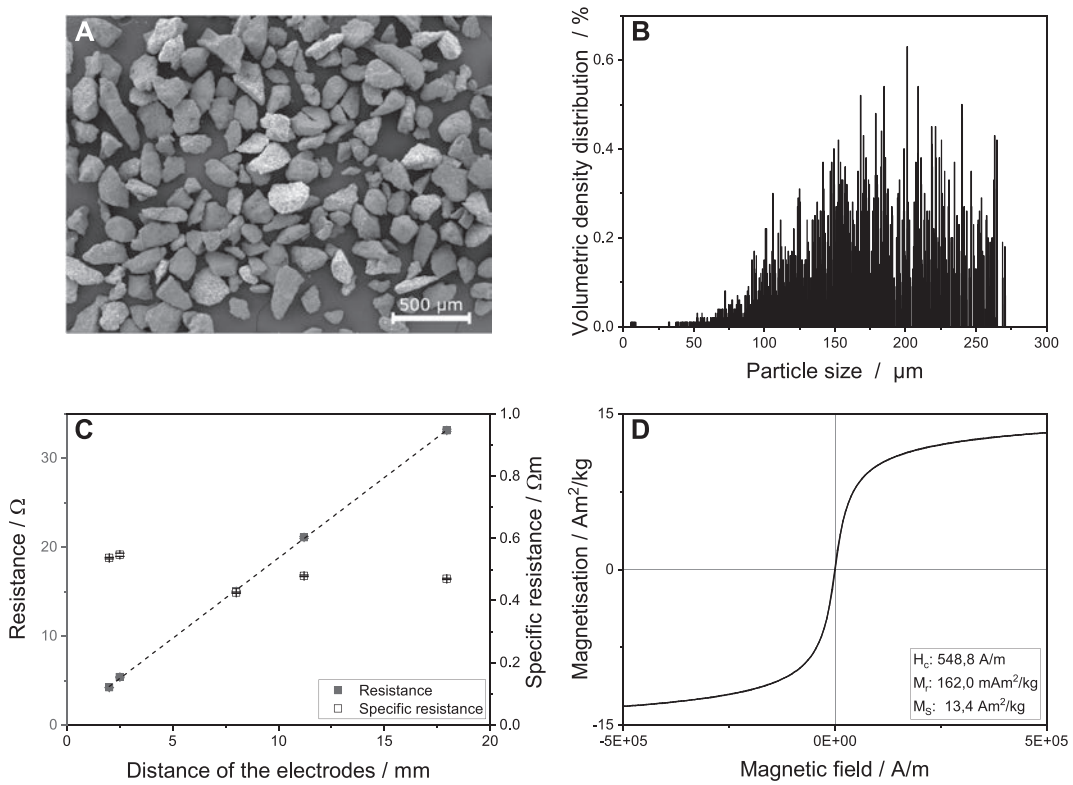

Fig. 1. A: Electron microscopy image of the used magnetic electrode particles. Magnification: 100. The particles show an irregular shape with a rough surface; B: Volumetric particle density distribution of the electrode particles. Based on the volume distribution the mean particle size is 175 µm; C: Specific resistance of dry electrode particles measured in a distance range from 2 to 18 mm between the working and counter electrode. The electrode particles show a pure ohmic behavior with an average specific resistance of 0.5 Ωm; D: Magnetization curve of the magnetic electrode particles [11]. The plot shows that the electrode particles have a saturation magnetization of 13.4 Am^2/kg, with a low remanence of 0.16 Am^2/kg.

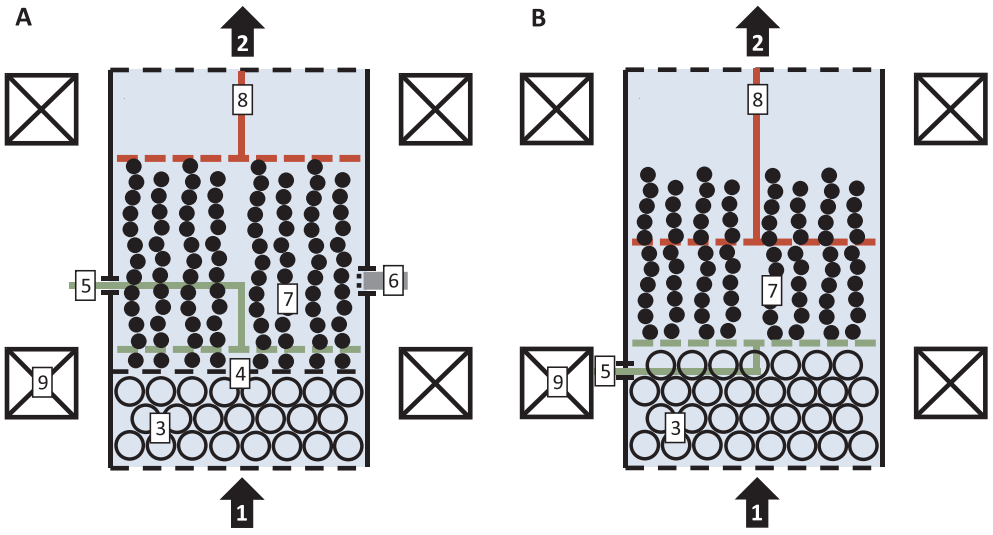

Fig. 2. Sketch of the working electrode arrangements used in the experiments. A: Arrangement of the working electrode for the electrochemical impedance studies (EIS). B: Arrangement of the working electrode for the DC chronoamperometry studies. 1: inflow direction of fluidization chamber; 2: outflow direction of fluidization chamber; 3: glass beads; 4: filter for retention of electrode particles; 5: stationary working electrode with current lead; 6: reference electrode; 7: magnetizable electrode particles; 8: counter electrode with current lead; 9: electric coil for generating the magnetic field.

Watson Marlow, Cheltenham, UK) and sealed by radial and axial seals. The reactor was connected to the pump system using standard fittings. A schematic illustration of the magnetically induced fluidized bed re actor is shown in Figs. 2 and 3B.

In the reaction chamber (19 mm inner diameter and 10 cm length) of the electrochemical fluidized bed reactor the working and counter electrode are localized. The working and counter electrode have the same dimensions and are made of platinized titanium with an electrode surface of 4 cm^2 each. The electrodes consist of a disc of 18 mm dia meter made from an expanded metal sheet by laser cutting. The used expanded metal sheet has a mesh size of 1.5 mm, and a strand thickness of 1 mm. A wire with a diameter of 1 mm was welded to the middle of the disc, serving as a current lead which can be connected to the po tentiostat. The counter electrode could be freely positioned in the re actor chamber, while the working electrode was installed at a fixed position. For better flow distribution, a short fixed bed of glass beads, having a diameter of 2 mm, was placed at the inlet of the reaction chamber.

The working electrode was positioned according to the type of ex periment (see Fig. 2). For the electrochemical impedance measurements (EIS), the working electrode was clamped into the bottom of the reac tion chamber. For this kind of experiments a three electrode

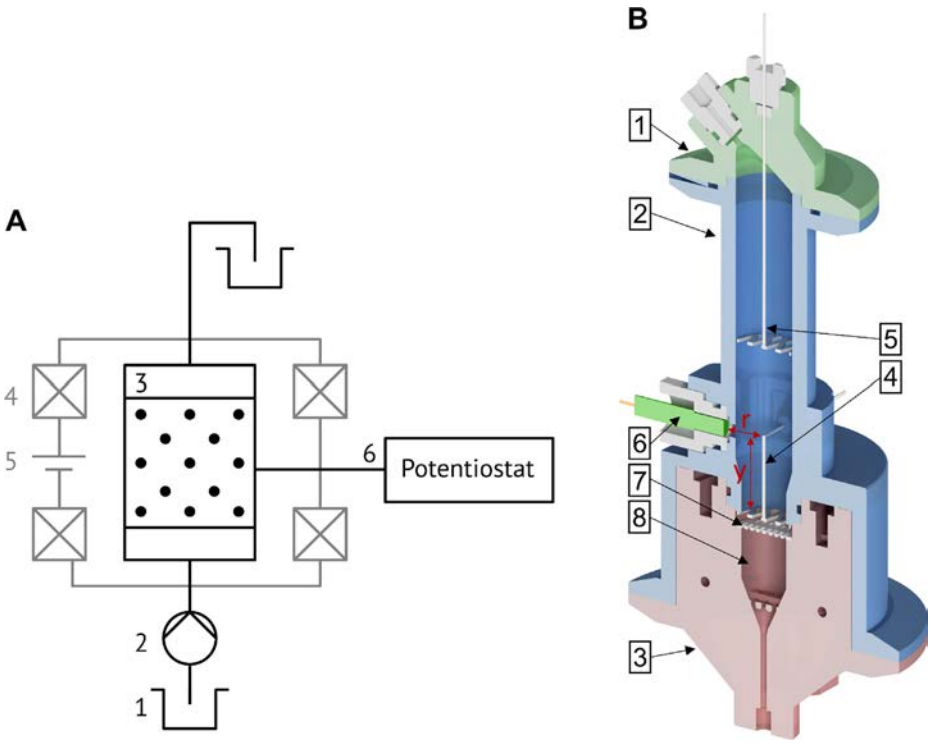

Fig. 3. A: Schematic illustration of the experimental setup; 1: reservoir of the reaction solution; 2: pulsation-free piston pump of the FPLC-System (Äkta purifier 100, GE Healthcare, Buckinghamshire, UK); 3: electrochemical reactor using a fluidized bed electrode; 4: Helmholtz arrangement of two electric coils placed around the reaction chamber to magnetically stabilize the fluidized bed electrode. The magnetic field is aligned in the direction of the fluid flow; 5: DC Power source for the electric coils; 6: Potentiostat (Interface 5000, Gamry, Warminster, USA); B: Schematic illustration of the magnetically stabilized fluidized bed reactor that was used for the electrochemical impedance spectroscopy; 1: upper reactor part; 2: reactor chamber; 3: lower reactor part; 4: stationary working electrode with current lead; 5: counter electrode with current lead; 6: reference electrode: the reference electrode was positioned with a radial distance r of 13 mm from the wire of the working electrode and a height y of 24 mm from the mesh of the stationary working electrode; 7: filter for particle retention; 8: reactor inlet filled with glass beads for flow distribution.

arrangement with a silver silver chloride reference electrode was used, having a radial distance of 13 mm to the platinized titanium wire ser ving as current lead of the stationary working electrode. The distance from the platinized expanded metal disc of the stationary working electrode was 24 mm. The distance to the electrode particles was 3 mm. The knowledge of these distances is important in order to estimate possible systematic errors in the impedance measurements resulting from the potential drop (iR drop) between the working electrode and the reference electrode. For the DC chronoamperometry studies, no reference electrode was used. Here the working electrode was placed in a way that the titanium wire serving as current lead did not contact the section of the particle bed placed between the working and the counter electrode.

2.3.2. Magnet module

Within the reaction chamber, the magnetic electrode particles can be influenced by the superposition of a magnetic field. For this, a Helmholtz coil system consisting of two individual coils was placed outside the reactor. Using the Helmholtz coil, DC magnetic flux den sities between 0 and 20 mT could be generated within the area of the fluidized bed. The coils were cooled during the entire process, so that no temperature increase could influence the process. The generated magnetic flux density was measured and controlled with a transverse Hall probe. The Hall probe was mounted on a FH 31 Gaussmeter from Magnet Physik Steingroever GmbH (Cologne, Germany).

2.4. Experimental set up

The magnetically stabilized fluidized bed reactor was connected to the pump of a FPLC (Fast Protein Liquid Chromatography) system (Äkta purifier 100, GE Healthcare, Buckinghamshire, UK). A potentiostat Interface 5000 from Gamry (Warminster, USA) was used for the Impedance and DC chronoamperometry studies. A schematic illustra tion of the experimental setup is shown in Fig. 3A.

2.5. Reactor operation

The investigations regarding the resistance of the fluidized bed electrode system with and without magnetic influence were carried out with DC chronoamperometric and impedance measurements. To flui dize the particle electrode, a 1 M sodium chloride solution was con tinuously pumped through the system as electrolyte. Before each ex periment, the solution was gassed with nitrogen in order to strip oxygen. In addition the high electrolyte concentration reduced the oxygen solubility [24]. All experiments were performed with a particle mass of 3 g and a constant flow rate of 1 respectively 2 mL/min. In previous investigations it could be shown that with this particle mass a uniform fluidization is possible [11].

2.5.1. Chronoamperometry studies

In the chronoamperometric studies, the ohmic resistance between the working and counter electrode was measured to determine the specific resistance of the fluidized bed electrode consisting of the par ticle phase and electrolyte phase (see Fig. 2B) [25]. A constant potential was applied between the two electrodes and the resulting current was recorded for the potentials -0.4 and -0.6 V until a steady state was reached. The corresponding specific resistance ρ was calculated with the ohmic law, the distance between the electrodes l and the cross section of the fluidized bed A (see Eq. (2.1)) [26]. With the chosen range, it was ensured that the applied potentials were smaller than the decomposition voltage of the electrolyte.

$$R = \rho \bullet \frac{l}{A} \tag{2.1}$$

For the resistance R measurements, the counter electrode was placed at different positions within the fluidized bed electrode. Here the current was recorded for the resulting distances of the counter electrode to the working electrode (the investigated distance range was between 4 and 15 mm). It should be mentioned that, in case of an ideal ohmic behavior, a linear relationship between distance and current is ex pected. In order to investigate the influence of the magnetic field on the resistance of the fluidized bed electrode, all experiments were per formed with and without the application of a magnetic field of 20 mT.

Furthermore, all experiments were carried out as triplets.

2.5.2. Electrochemical impedance spectroscopy (EIS) studies

The electrochemical impedance spectroscopy (EIS) was performed using the three electrode arrangement (see Fig. 2A). The investigated frequency range was between 10 kHz − 9 mHz and the AC amplitude was 10 mV. The experimental data were fitted using the Gamry Echem Analyst software from Gamry (Warminster, USA).

3. Results and discussion

3.1. Chronoamperometric studies of the magnetically stabilized fluidized bed electrode

The most basic method of investigating the resistance behavior of a fluidized bed electrode can be achieved by means of DC voltage measurements between two electrodes [25]. For this purpose, it must be ensured that an electrical conduction path between the working and counter electrode is possible and that no side reactions occur. The absence of side reactions means, that the electrical potential between the working and the counter electrode is lower than the required potential of all relevant redox reactions in the electrolyte solution. The most relevant redox reactions in our simple 1 M NaCl solution are water electrolysis and the reduction of dissolved oxygen. The investigations were carried out at flow rates of 1 and 2 mL/min respectively, with the particle bed expanding by 9 and 16%. To observe the magnetic influence on the resistance behavior, the electrode bed was superimposed by a magnetic field of 20 mT. In the case of the superposition of a magnetic field, the expansion of the particle bed was reduced to 6 and 13% at the flow rates of 1 and 2 mL/min. The results of the test series are presented in Fig. 4 and were carried out in triple determination.

For the experiments shown in Fig. 4A, as already mentioned, the counter electrode was positioned in the fluidized particle bed and the resistance of the bed was determined in dependence of the distances from the working electrode. Despite a gentle pressure applied to the counter electrode while the flow was switched on, the distance between the electrodes could not be reduced below approx. 4 mm. We assume that at this short distance the fluidized state could not develop and a thin layer of particles is compressed between the electrodes. Starting from this minimal distance and carefully increasing the distance stepwise, a short region could be reproducibly observed in which the resistance stayed at a low level of 100 200 Ω and only increased slowly with increasing distance. As will be discussed in more detail in Section 3.2.2.1, this region is dominated by charge transfer along uninterrupted particle chains directly connecting the two electrodes. From our results, it can be estimated that in case of the used electrode particles with an average diameter of 175 μm, these particle chains can show a length of up to around 6 mm. This number is in excellent accordance to the effective chain length of 5 mm which was determined independently in an electrochemically active fluidized bed of the same particle type [11]. In this case, the chain length was calculated on the basis of the achieved electrochemical conversion rates and the specific particle surface. At distances beyond 6 mm, the slope of the resistance curve changes remarkably and a second region of the charge transport within a fluidized bed can be identified. Up to the maximum distance realizable in our setup, a steep but constant slope can be observed, resulting in resistances of more than 10 kΩ at 15 mm distance. The linear relationship can easily be explained by Ohm's law, which says that in case of a constant voltage the current is proportional to the ohmic resistance of a given system. A constant slope, corresponding with a constant specific resistance of the fluidized bed, can be observed for both investigated flow rates as well as without and with the influence of the magnetic field, however the absolute values of the specific resistances vary.

The results in Fig. 4A show that with a higher flow rate the specific resistance of the fluidized particle system increases. This characteristic could already be shown in previous publications [5,27]. Furthermore, the expansion of the particle bed was described by Sabacky [5] and Kusakabe [27] as the main variable that influences the conductivity of the particle bed. However, a new approach is the magnetic stabilization of the fluidized bed electrode. Fig. 4A shows that the total resistance of the electrode can be reduced by superposing the fluidized bed electrode magnetically. To get a better overview of the improvement of the electrical resistance by means of the magnetic field, the specific resistance was calculated for the results of Fig. 4A and is shown in Fig. 4B. The specific resistance of the fluidized bed electrode is a constant value that is independent of the electrode distance and changes according to the flow rate and magnetic influence. The specific resistances shown in Fig. 4B illustrate more clearly the influence of the flow rate and the magnetic field. When the average specific resistances for the flow rates 1 and 2 mL/min are considered, it increases with the higher flow rate from 336 to 345 Ωm. If the fluidized bed electrode is superposed with a magnetic field of 20 mT, the specific resistance is reduced at a flow rate of 1 mL/min from 336 to 285 Ωm and at a flow rate of 2 mL/min from 345 to 326 Ωm. Here it is also shown that the effect of the magnetic field decreases with an increase in the flow rate, so that at a flow rate of 1 mL/min an improvement in the specific resistance of 15% and at a

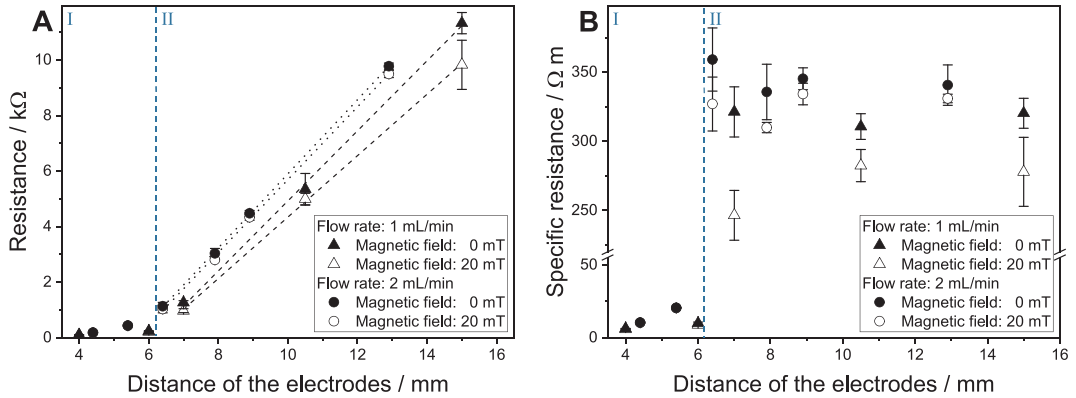

Fig. 4. A: Ohmic resistance measured within the fluidized bed electrode with and without superimposed magnetic field at varying distance of the electrodes. The resistance curve shows two clearly distinguishable regions, with a low and only slightly increasing resistance at short electrode distances (region I) and a high but constant slope at higher electrode distances (region II). The distance of 4 mm represents the smallest achievable distance between the electrodes, with a small amount of compressed particles still in between. Higher flow rates result in a steeper slope of the resistance values, while the application of a magnetic field of 20 mT resulted in a slightly decreased resistance. B: Specific resistance of the fluidized bed electrode in the distance range from 4 to 15 mm between the working and counter electrode. At a flow rate of 1 mL/min (9% bed expansion compared to the settled state) the application of a magnetic field reduces the specific resistance from around 336 Ωm at 0 mT to around 285 Ωm at 20 mT.

flow rate of 2 mL/min of 6% is achieved.

When comparing the findings listed above with the specific resistance of 0.5 Ωm measured in a gently pressed bed of dry particles (see Fig. 1C), it is also apparent that the specific resistance in the fluidized bed is several orders of magnitude higher. If only the electrical resistivity of pure activated carbon (approx. 0.05 Ωm) [28] is considered, it also becomes noticeable that the electrical conductivity of our composite particles is already reduced by a factor of around ten if compared with the one of pure activated carbon. Here it must be mentioned, that the electrical resistance of activated carbon is only a reference value and of course varies depending on the type used. In region I of Fig. 4A, a 10 fold higher value of 5.7 Ωm is shown at a flow rate of 1 mL/min and a magnetic field of 20 mT. If we try to compare our values with the ones of other fluidized bed electrodes reported in literature, another interesting point emerges. Sabaky also investigated the electrical resistivity of his particles in different expansion states in his studies [5]. Also in comparison with Sabaky's results, our particles show significantly higher resistivity values. At similar expansion states, Sabacky could measure values from 0.01 to 0.05 Ωm, depending on the particle size used. Here, the specific resistances determined are largely influenced by the particle material, which consisted of copper, but also by the almost spherical shape of his particles.

In summary it can be said, that in case of the chronoamperometric studies a magnetic field of 20 mT superimposed to the fluidized bed, does not result in strong changes of its specific resistance if the electrode distance exceeds 6 mm. At first sight, this seems contradictory to the results of our previous study [11], in which we showed that at a flow rate of 1 mL/min, the superposition of a magnetic field of 20 mT onto the fluidized bed electrode leads to a 100% improvement in the electrochemical conversion. However, one has to keep in mind, that we also showed that the electrochemical conversion only took place in a small part of the fluidized bed being close to the working electrode and corresponding with an effective chain length of a few millimeters. As written above, this part of the fluidized bed corresponds with region I in Fig. 4A. However, the discussed specific resistances belong to region II in Fig. 4A, corresponding with a larger electrode distance and a convective instead of a conductive charge transfer (see Section 3.2.2.1). These results indicate, that on the one hand the superimposition of a magnetic field is less effective in region II, resulting in an only slight reduction of the specific resistance by 15%. On the other hand, the high specific resistance in region II leads to a fast drop of the electric potential in this part of the fluidized bed, which is why only the particles in the close proximity (region I) of the working electrode will participate in an electrochemical reaction. In the next section, we discuss the results of EIS studies which we conducted to get a better insight of charge transfer processes in this region and how a magnetic field influences these processes.

3.2. EIS studies of a magnetically stabilized fluidized bed electrode

There are only few published studies that describe the dynamic behavior of a fluidized bed electrode using electrochemical impedance spectroscopy (EIS) measurements. EIS investigations on a magnetically stabilized fluidized bed electrode have not yet been performed. For a better understanding of the behavior of such a system, several parameters have been investigated. Studies have been carried out describing the magnetic influence on the fluidized bed electrode and the influence of the flow rate on the magnetically superimposed fluidized bed electrode (see Fig. 5A and B).

3.2.1. Influence of the flow rate and magnetic superposition

For the EIS studies the two electrode arrangement of the chronoamperometric studies was replaced by a three electrode arrangement including a reference electrode (see Section 2.3). Again, a particle mass of 3 g was used for all experiments and the strength of the magnetic field was varied from 0 to 20 mT, while all other parameters were kept constant. In Fig. 5A the results of the magnetic field variation were plotted in case of a constant flow rate of 1 mL/min (9% bed expansion). In addition, EIS measurements were carried out without fluidization, saying for a fixed bed electrode for comparison purposes.

Looking at the results plotted in Fig. 5A and B, the different electrode states caused by fluidization and magnetic influence result in significant changes in the Nyquist plot of the EIS measurements. First of all, at very high frequencies, a constant resistance is observed which can be determined at $Z''(\omega) = 0$. This constant offset is mainly caused by the resistance of the current leads and the ionic resistance of the electrolyte [29,30].

Depressed semicircles could be identified for all test series. In the EIS measurements of the fixed bed the smallest semicircle was found. With the fluidization of the electrode bed, the diameter of the semicircle increases significantly and stretches from high up to intermediate frequencies in the range of 1 Hz. Gabrielli [1] observed the same characteristics in case of a conventional fluidized bed and showed that the increase of the semicircle is caused by a decrease of the contacting of the electrode particles at higher flow rates [1,19]. The same explanation holds for the increase of the semicircle during the fluidization of the electrode particles in our case. However, in the case of the superposition of a magnetic field onto the fluidized bed, the depressed semicircles become smaller again, meaning that the contacting within the fluidized bed can be described as being between the fluidized and fixed bed status. As a result, with a magnetic influence of 0, 10 and 20 mT, the diameter of the depressed semicircle changes from 41 Ω to 35 and 29 Ω. Here the influence of the superimposed magnetic field of 20 mT shows a reduction of the contacting resistance of the electrode particles up to 42% of the initial value. However, the interpretation of the parameters of the semicircle has to be done with care, because in the high frequency range it is influenced by the metal electrode as well. A better indicator of the improved conductivity in case of the application of a magnetic field is the strong decrease of the imaginary impedance at very low frequencies (9 mHz). The reciprocal of this values correlates with effective capacity during the impedance measurements. Comparing the reciprocal values at 0 and 20 mT a rough estimation shows that the effective capacity increases around 100% when the magnetic field is applied (a more detailed analysis of the involved resistances and capacitances can be found in Section 3.2.2.2). In order to explain this capacity increase, it can be assumed that more particles get in direct contact with the electrode and get charged during the long periods at a positive or negative potential of a sinusoidal voltage at 9 mHz. This increase of the directly contacted particles corresponds well with the charge transport via conductive particle chains which is assumed in close proximity to the electrode (region I in Fig. 4A and the related discussion). Therefore, it can be said that while the chronoamperometric resistance is influenced by the complete fluidized bed located between the working and counter electrode, the result of the EIS measurements is mainly influenced by the local particle arrangement close to the working electrode.

Another aspect that needs to be considered is the porosity of the particles of the fluidized bed. The particles consist to a large extent of activated carbon. When an electric potential is applied to the particles, ions of the electrolyte accumulate in the so called electrical double layer at the large inner surface of the porous particles [29]. This effect manifests in the depressed course of the semicircles [31,32] and especially in the observed high capacities notable in the EIS measurements. The low frequency range of the Nyquist plot is characterized by an almost straight line following the first semicircle (Fig. 5A). The straight line having a slope around 45° is a clear indication of a combined diffusion and accumulation process of the ions within a porous electrode material [31,33]. If we compare the results with Gabrielli's [1,19] studies, we notice, that the lines in our work do not merge into a vertical line in the lower frequency range as it is the case in Gabrielli's studies for electro inactive fluidized beds. The reasons for this difference are: (i) The inner surface and therefore the capacity of our porous

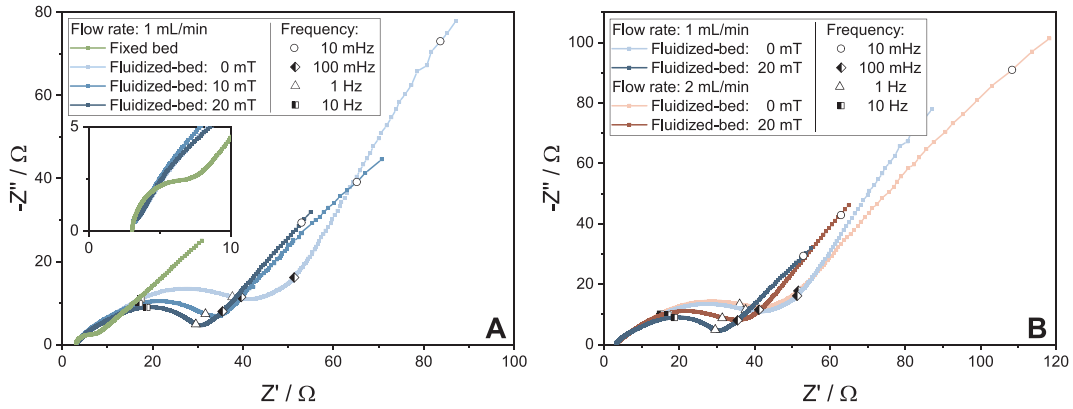

Fig. 5. Results of EIS measurements of the magnetically stabilized fluidized bed electrode; Investigated frequency range from 0.009 Hz to 10 kHz for different flow rates and magnetic field strengths. The Figures show the resulting Nyquist plots, saying the real part Z''(ω) of the impedance plotted versus the imaginary part Z'(ω); A: EIS measurements at a flow rate of 1 mL/min and the magnetic field strengths of 0, 10 and 20 mT. The Nyquist plot of an EIS measurement in a fixed bed is also shown for comparison. Here the flow direction was reversed and a flow rate of 1 mL/min was used. As the magnetic field strength increases from 0 to 20 mT, the size of the first semicircle and the imaginary impedance at low frequencies are strongly reduced. B: Comparison of the EIS measurements for the flow rates 1 and 2 mL/min and the magnetic field strength of 0 and 20 mT; particle amount: 3 g.

particles is much larger than the capacity of the non porous, gold plated particles used in Gabrielli's work. Therefore, while the capacity of Gabrielli's particles is fully charged at low frequencies resulting in a vertical line in the Nyquist plot the capacity of our particles does not show that it reaches its limits even at the lowest frequency of 0.009 Hz, which is lower than the lowest one used by Gabrielli [1]. (ii) The po sition of the counter electrode differs in our studies from the position used by Gabrielli. In Gabrielli's work the counter electrode was located above the fluidized particle bed, while in our case the counter electrode was place at the upper rim of the fluidized bed but still staying in contact with fluidized particles. The effect of this difference can be il lustrated best by discussing the extreme case of an infinitely long period of the voltage signal, which is equivalent to a DC signal. In the absence of electrochemical reactions, the arrangement of Gabrielli equals a plain capacitor showing a vertical line in the Nyquist plot. In contrast, our arrangement allows a small but permanent current in the DC case, caused by the convective charge transport discussed above. Therefore, for very low frequencies our system equals a parallel RC element with a large ohmic resistance R. As a result, there is no vertical line in the low frequency range, but rather the beginning of a very large second semicircle indicated by a slight concave bending of the line.

In addition to the variation of the magnetic field strength, it was also investigated how a higher flow rate in the EIS measurement be haves at a magnetic field strength of 0 and 20 mT. In Fig. 5B the results of experiments at a flow rate of 1 and 2 mL/min are compared. In principle, the Nyquist plots of experiments at a flow rate of 2 mL/min show similar characteristics than the test series at a flow rate of 1 mL/min. However, the depressed semicircles in the high and intermediate frequency range show a larger diameter, indicating an inferior contact between the particles as well as between the particles and the current source.

3.2.2. Equivalent electric circuit model of a fluidized particle electrode

Gabrielli has already developed an equivalent circuit model of a fluidized particle electrode in his studies [1]. However, his equivalent circuit is based on a transmission line model, which has a high com plexity. In order to gain a model which takes into account the non idealities of porous particles and the different counter electrode ar rangement of our setup, we developed an equivalent circuit which is mainly based on so called constant phase elements, which requires a strongly reduced amount of circuit elements (see Fig. 6).

All experimental data could be fitted with the developed model with a high degree of validity. Here, the square of the calculated sum of the weighted residuals of the resulting fits was for all experimental results in the range of 10^{-4}. The experimental results were fitted by using the software Gamry Echem Analyst (Gamry Instruments, USA). An example of a fitted plot can be found in SI Fig. S1. The equivalent circuit ele ments in Fig. 6 represent the charge transfer between the current source and the electrode particles (1), the conductive charge transfer between electrode particles directly connected within a particle chain (3), the convective charge transfer between charged and uncharged particles that have no direct contact (5) and the resistances resulting from the electrolyte and the current leads (7).

3.2.2.1. Charge transfer at the current source and between the electrode particles. Sabacky [5] presented the conductive charge mechanism as one of the main mechanisms responsible for the charge transport within the fluidized bed. Here, the charge is transferred by direct contact of the particles with the surface of the metal electrode as well as with other particles, which themselves are in direct contact with the electrode. Besides the resistance of the direct electrode particle and particle particle contact, the capacity of the electric double layer at the electrode and particle surfaces influences the frequency dependence of the impedance of the system. At high and intermediate frequencies, the period of the sinusoidal voltage signal is too short for the ions to diffuse longer distances into the inner structure of the porous particles. Therefore, in first approximation only the electrode surface and the outer surface of the directly contacted particles contribute to the effective capacity in this frequency range. The interplay of the conductive resistance and the charging/discharging of this capacity leads to a semicircle in the Nyquist plot. The same parallel R C impedance behavior is known from other porous conductive systems such as double layer capacitors [30], carbon flow electrodes [21] and conventional fluidized bed electrodes [1,19,20,22,23]. In our equivalent circuit model, we distinguish between the first R C element formed by the metal electrode itself and the second R C element involving the outer regions of porous particles which are in direct contact with the electrode. The first R C element can be assigned to the high frequency range and has ideal capacitive properties because of the non porous electrode surface. Instead of an ideal R C element, we use a constant phase element (CPE) for the description of the capacitance in the second section of our equivalent circuit model. The non ideal capacitive behavior of porous materials results in depressed semicircles in Nyquist plots [31 33]. It should be mentioned, that the Nyquist plots of the EIS measurement of our fluidized bed reactor does not show a clear distinction between the first R C and the following R CPE element, and the distinction in the model serves more for

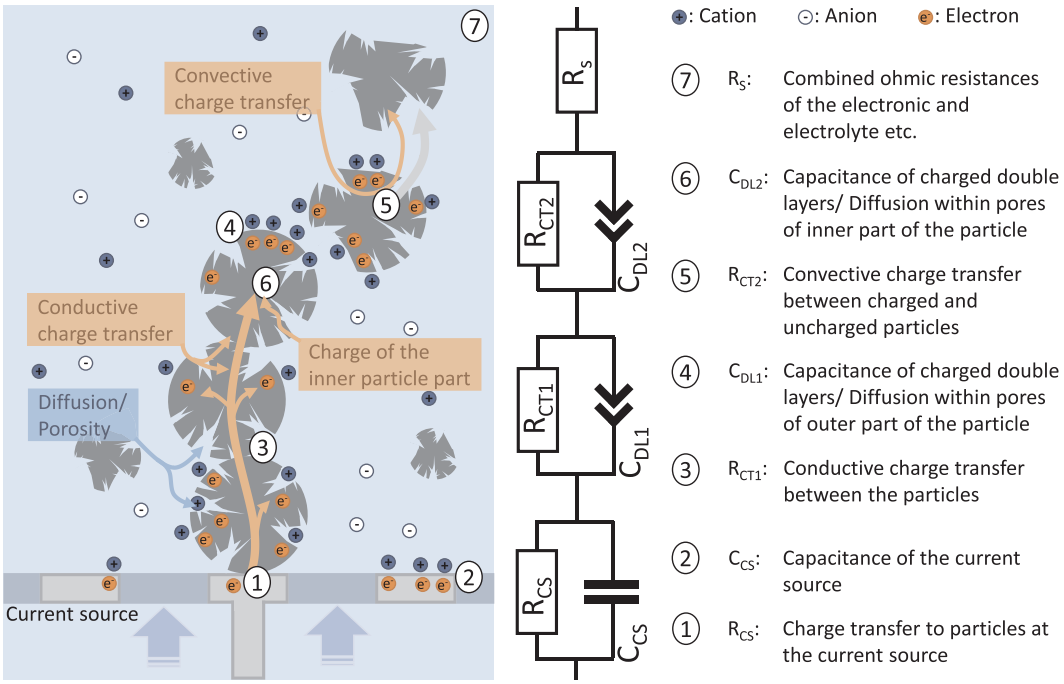

Fig. 6. Principle sketch of the charge transfer in a fluidized bed electrode and the underlying equivalent circuit model.

visualization and generalization purposes.

Finally, a third R C respectively R CPE element is integrated into our equivalent circuit model. It describes the charging of the inner part of the porous particles at low frequencies < 1 Hz. The charging pro cess is characterized by the diffusion of ions of the electrolyte within the particle pores and the associated accumulation of the ions in the electric double layer of the micropores which are connected to the meso and macropores in which the diffusion takes place [30]. The EIS response of such a combined diffusion/accumulation process can be described by a CPE element having an exponent around 0.5 [21,31,33,34]. The third CPE is also placed parallel to a resistor re presenting mainly the conductive charge transfer between the particles. Particles at larger distances connected by convective charge transfer contribute only minor to the total current measured during the EIS studies, because the current path between the working electrode and these particles is characterized by high resistances in the kΩ range (see Fig. 3A). Therefore, the shape of the Nyquist plot is dominated by the local fluidized bed around the working electrode, corresponding with region I when referring to the discussion of the chronoamperometric studies (see Fig. 4A).

3.2.2.2. Review of the parameters fitted to the equivalent circuit model of the EIS studies. The data of the EIS measurements were fitted with the model described in the section before (see Table 1). The fitted data show how the applied flow rate and the magnetic influence on the fluidized bed electrode affects the resistance and capacitance values. In case of CPE elements, the corresponding capacitance is calculated from the CPE parameters as described in the SI (see Eq. (S.1)).

Table 1
Parameters fitted to the equivalent circuit model of the EIS studies.

Flow rate:	1 mL/min						
Magnetic field (mT):	R_S (Ω)	R_{CS} (Ω)	C_{CS} (mF)	R_{CT1} (Ω)	C_{DL1} (mF)	R_{CT2} (Ω)	C_{DL2} (F)
0	2.9	8.3	5.4	37.5	1.1	1166	0.5
10	2.9	7.9	3.8	23.5	0.7	550	1.4
20	3.0	8.3	2.6	19.3	0.4	523	2.2
Flow rate:	2 mL/min						
Magnetic field (mT):	R_S (Ω)	R_{CS} (Ω)	C_{CS} (mF)	R_{CT1} (Ω)	C_{DL1} (mF)	R_{CT2} (Ω)	C_{DL2} (F)
0	3.0	8.1	7.0	37.6	1.6	1220	0.48
20	3.0	7.8	3.9	24.9	1.0	530	1.02

As expected, the resistance R_S caused by the current leads and the ionic resistance of the electrolyte is practically constant with a value of 3 Ω in all experiments.

As already mentioned, in an idealized picture the first semicircle represents the inner resistance and the capacity of the metallic elec trode. This picture is backed by the observation that there is no change in the resistance values R_{CS} when superposing a magnetic field or switching to higher flow rates. The resistance remains almost constant at a value of 8 Ω at a flow rate of 1 and 2 mL/min and in the in vestigated magnetic field strength range of 0 to 20 mT. However, the fitted capacity values of C_{CS} are in the mF range, while they were ex pected to be around 100 μF assuming an electrode surface of 4 cm^2 and a specific capacitance of the metal electrode of 25 μF/cm^2 [35]. Therefore, we assume that the resistance value R_{CS} as well as the ca pacitance C_{CS} is not only related to the electrode but also of the first layer of particles being in direct contact to the electrode. Although rather speculative, this may also explain why the fitted C_{CS} shows a decreasing tendency when a magnetic field is applied. As the illustra tion in Fig. S2 of the SI shows, while the application of a magnetic field increases the total number of particles staying in contact with the electrode surface via long chains, the ordered arrangement may reduce the number of particles directly touching the electrode.

If we look at the fitted parameters representing the outer (R_{CT1}/C_{DL1}) and inner (R_{CT2}/C_{DL2}) shells of the particles connected to the electrode via particle particle contacts along more or less extended chains, a different behavior is shown. Here the resistances decrease when a magnetic field is applied, while they stay practically constant when the flow rate is increased from 1 to 2 mL/min. This illustrates the direct influence of the magnetic field on the conductive particle particle contact, which takes place in the proximity of the current source. The magnetic particles form magnetic dipoles and attract each other. As a consequence, they align along the magnetic field lines and show an improved particle particle contact with each other. A stronger magnetic field also has a greater influence on the observed resistance. At a flow rate of 1 mL/min and a magnetic field of 10 and 20 mT, the resistance R_{CT1} is reduced by 37 and 49%. The resistance R_{CT2} shows the same dependencies, with a reduction of 55% at a flow rate of 1 mL/

min and comparing the fitted values in case of the experiment with 0 and 20 mT respectively. The effect of the magnetic field is even more pronounced when looking at the fitted parameter C_{DL2} which represents the sum of the capacity of the inner shells of all particles staying in contact with the electrode via direct particle chains. Therefore, in contrast to the resistance parameter R_{CT2} which is a measure of the strength of the particle particle contact, the capacity parameter C_{DL2} is a rough measure of the total number of particles which stay in contact with the electrode. Looking at the C_{DL2} values in Table 1, it shows that at a flow rate of 1 mL/min the application of a magnetic field of 20 mT increases the value of C_{DL2} by more than the factor four. If the flow rate is set to 2 mL/min, the effect of a magnetic field of 20 mT results in an increase of C_{DL2} of only a factor of two, showing that the formation of particle chains is quickly disturbed in case of higher flow rates. At the end it should be mentioned that the usefulness of EIS measurements and our equivalent circuit model can be nicely shown when comparing the determined factors of C_{DL2} with and without the application of a magnetic field with the effective electrode surface of our reactor in case of electrochemical conversions (see Fig. 9 of Ref. [11]). In our recent studies on electrochemical reactions in a fluidized bed reactor, we found, that using the same particles and the same particle amount, the particle surface being effective in the reaction could be substantially increased by the application of a magnetic field of 20 mT. In case of a flow rate of 1 mL/min the effective surface (correlating with the number of effective particles) was increased by a factor of four, in case of 2 mL/min the factor was reduced to two. Therefore, the determined factors are practically identical with the ones determined for the effective capacity C_{DL2}, showing the usefulness of fast and easy to conduct EIS measurements for the prediction of the effectiveness of a particle based electrochemical reactor.

4. Summary and conclusion

In this study, we investigated the electrical conductivity within a magnetically stabilized fluidized bed electrochemical reactor with a 3D particle electrode. In this type of reactor, the electrode surface is enlarged with magnetic electrode particles in order to improve the electrochemical yield, e.g. during electrochemical conversion reactions. The contacting of the fluidized electrode particles is improved by means of a superimposed magnetic field. In order to investigate the electrical resistance of the magnetically influenced fluidized bed electrode, chronoamperometric and EIS measurements were carried out chronoamperometric studies measuring the ohmic resistance in the complete fluidized bed located between two electrodes revealed that a magnetic field of 20 mT does not show a strong impact. At a flow rate of 1 mL/min and a particle mass of 3 g, the magnetic influence could improve the electrical resistivity by only 15%. In contrast, the region of the fluidized bed recorded by EIS measurements is frequency depended and restricted to relatively small distance around the working electrode. Here a magnetic field of 20 mT applied at a flow rate of 1 mL/min resulted in a decrease of the resistance of the conductive particle particle contact by up to 49%. Even more pronounced is the effect of the magnetic field in case of the apparent electric capacity of the fluidized bed in close proximity to the working electrode. The apparent electric capacity, corresponding with the amount of particles effectively coupled to the working electrode, shows an increase of approx. 400%. This factor could also be determined when calculating the charge accumulated by the electrode particles in the chronoamperometric experiments (see SI Fig. S3). This value is in good agreement with our previous study, in which we investigated the influence of a superposed magnetic field onto the effective electrode surface participating in the electrochemical reaction. Therefore, this work demonstrates the benefits of a magnetizable fluidized particle electrode and the usefulness of easy to conduct EIS studies for the prediction of the performance enhancement, which can be gained by the application of an external magnetic field.

Declaration of Competing Interest

The authors declare that they have no known competing financial interests or personal relationships that could have appeared to influence the work reported in this paper.

Acknowledgements

The authors acknowledge financial support from the German Federal Ministry of Education and Research within the priority program “Elektrowirbel” (FKZ: 13XP5008E).

References

[1] C. Gabrielli, et al., Dynamic Analysis of Charge Transport in Fluidized-Bed Electrodes - Impedance Techniques for Electroinactive Beds, J. Appl. Electrochem. 22 (9) (1992) 801–809.
[2] D. Hutin, F. Coeuret, Experimental-Study of Copper Deposition in a Fluidized-Bed Electrode, J. Appl. Electrochem. 7 (6) (1977) 463–471.
[3] J.N. Hiddleston, A.F. Douglas, Current/Potential Relationships and Potential Distribution in Fluidized Bed Electrodes, Electrochim. Acta 15 (3) (1970) p. 431-+.
[4] Berent, T., R. Mason, and I. Fells, Fluidised-Bed Fuel/Cell Electrodes. Journal of Applied Chemistry and Biotechnology, 1971. 21(3): p. 71-&.
[5] B.J. Sabacky, J.W. Evans, Electrical-Conductivity of Fluidized-Bed Electrodes - Significance and Some Experimental Measurements, Metall. Trans. B-Process Metallurgy 8 (1) (1977) 5–13.
[6] G. Kreysa, S. Pionteck, E. Heitz, Comparative Investigations of Packed and Fluidized-Bed Electrodes with Non-Conducting and Conducting Particles, J. Appl. Electrochem. 5 (4) (1975) 305–312.
[7] K. Kazdobin, N. Shvab, S. Tsapakh, Scaling-up of fluidized-bed electrochemical reactors, Chem. Eng. J. 79 (3) (2000) 203–209.
[8] M. Fleischmann, J. Oldfield, L. Tennakoon, Fluidized bed electrodes Part IV. Electrodeposition of copper in a fluidized bed of copper-coated spheres, J. Appl. Electrochem. 1 (2) (1971) 103–112.
[9] M. Fleischmann, J.W. Oldfield, Fluidised Bed Electrodes. 1. Polarisation Predicted by Simplified Models, J. Electroanal. Chem. 29 (2) (1971) p. 211-+.
[10] M. Fleischmann, J.W. Oldfield, Fluidised Bed Electrodes. 2. Effective Resistivity of Discontinuous Metal Phase, J. Electroanal. Chem. 29 (2) (1971) p. 231-+.
[11] A. Tschöpe, et al., A Magnetically Induced Fluidized-bed Reactor for Intensification of Electrochemical Reactions, Chem. Eng. J. 385 (2020).
[12] R. Hausmann, et al., Mass transfer rates in a liquid magnetically stabilized fluidized bed of magnetic ion-exchange particles, Chem. Eng. Sci. 55 (8) (2000) 1477–1482.
[13] J.Y. Hristov, Fluidization of ferromagnetic particles in a magnetic field.1. The effect of field line orientation on bed stability, Powder Technol. 87 (1) (1996) 59–66.
[14] M.J. Espin, M.A.S. Quintanilla, J.M. Valverde, Magnetic stabilization of fluidized beds: Effect of magnetic field orientation, Chem. Eng. J. 313 (2017) 1335–1345.
[15] K. Mandel, et al., Synthesis and stabilisation of superparamagnetic iron oxide nanoparticle dispersions, Colloids Surf A Physicochem Eng Asp 390 (1–3) (2011) 173–178.
[16] M.A. Burns, D.J. Graves, Structural Studies of a Liquid-Fluidized Magnetically Stabilized Bed, Chem. Eng. Commun. 67 (1988) 315–330.
[17] J. Backhurst, et al., A preliminary investigation of fluidized bed electrodes, J. Electrochem. Soc. 116 (11) (1969) 1600–1607.
[18] J.S. Newman, C.W. Tobias, Theoretical Analysis of Current Distribution in Porous Electrodes, J. Electrochem. Soc. 109 (12) (1962) 1183–1191.
[19] C. Gabrielli, et al., Dynamic Analysis of Charge-Transport in Fluidized-Bed Electrodes - Impedance Techniques for Electroactive Beds, J. Appl. Electrochem. 24 (6) (1994) 481–488.
[20] C. Gabrielli, B. Tribollet, A Transfer-Function Approach for a Generalized Electrochemical Impedance Spectroscopy, J. Electrochem. Soc. 141 (5) (1994) 1147–1157.
[21] A. Rommerskirchen, et al., Unraveling charge transport in carbon flow-electrodes: Performance prediction for desalination applications, Carbon 145 (2019) 507–520.
[22] T. Huh, J.W. Evans, Electrical and Electrochemical-Behavior of Fluidized-Bed Electrodes. 2. Effective Bed Resistivities, J. Electrochem. Soc. 134 (2) (1987) 317–321.
[23] T. Huh, J.W. Evans, Electrical and Electrochemical-Behavior of Fluidized-Bed Electrodes. 1. Potential Transients and Time-Averaged Values, J. Electrochem. Soc. 134 (2) (1987) 308–317.
[24] R. Battino, T.R. Rettich, T. Tominaga, The Solubility of Oxygen and Ozone in Liquids, J. Phys. Chem. Ref. Data 12 (2) (1983) 163–178.
[25] R.B. Macmullin, G.A. Muccini, Characteristics of Porous Beds and Structures, AIChE J. 2 (3) (1956) 393–403.
[26] D.S. Liu, C.Y. Ni, A thermo-mechanical study on the electrical resistance of aluminum wire conductors, Microelectron. Reliab. 42 (3) (2002) 367–374.

[27] K. Kusakabe, S. Morooka, Y. Kato, Charge-Transfer Rate in Liquid-Solid and Gas-Liquid-Solid Fluidized-Bed Electrodes, J. Chem. Eng. Jpn. 14 (3) (1981) 208–214.
[28] A. Barroso-Bogeat, et al., Electrical conductivity of activated carbon-metal oxide nanocomposites under compression: a comparison study, PCCP 16 (45) (2014) 25161–25175.
[29] C.Z. Yang, et al., Complex Impedance with Transmission Line Model and Complex Capacitance Analysis of Ion Transport and Accumulation in Hierarchical Core-Shell Porous Carbons, J. Electrochem. Soc. 160 (4) (2013) H271–H278.
[30] S. Yoon, C.W. Lee, S.M. Oh, Characterization of equivalent series resistance of electric double-layer capacitor electrodes using transient analysis, J. Power Sources 195 (13) (2010) 4391–4399.
[31] R.D. Levie, On porous electrodes in electrolyte solutions: I. Capacitance effects, Electrochimica Acta 8 (10) (1963) 751–780.
[32] R.D. Levie, The influence of surface roughness of solid electrodes on electrochemical measurements, Electrochim. Acta 10 (2) (1965) 113–130.
[33] J. Bisquert, et al., Impedance of constant phase element (CPE)-blocked diffusion in film electrodes, J. Electroanal. Chem. 452 (2) (1998) 229–234.
[34] Epelboin, I., Faradaic Impedances - Diffusion Impedance and Reaction Impedance. Journal of the Electrochemical Society, 1970. 117(8): p. 1052-&.
[35] J. Goodisman, Charging of the Liquid-Metal Surface and the Capacitance of the Metal Electrolyte Interface, J. Chem. Phys. 90 (10) (1989) 5756–5763.